한국소음진동공학회 2011년 추계학술대회논문집, pp.236~241

Detailed Design of an Active Rotor Blade for Reducing Helicopter Vibratory Loads

Balakumaran Natarajan†, WonJong Eun* and SangJoon Shin*

Key Words: Active rotor blade, Active Trailing-edge Flap (ATF), Piezoelectric actuator, Vibration control.

ABSTRACT

An active trailing-edge flap blade named as Seoul National University Flap (SNUF) blade is designed for reducing helicopter vibratory loads and the relevant aeroacoustic noise. Unlike the conventional rotor control, which is restricted to 1/rev frequency, an active control device like the present trailing-edge flap is capable of actuating each individual blade at higher harmonic frequencies i.e., higher harmonic control (HHC) of rotor. The proposed blade is a small scale blade and rotates at higher RPM. The flap actuation components are located inside the blade and additional structures are included for reinforcement. Initially, the blade cross-section design is determined. The aerodynamic loads are predicted using a comprehensive rotorcraft analysis code. The structural integrity of the active blade is verified using a stress-strain recovery analysis.

Nomenclature

c	=	blade chord length
c_f	=	flap chord length
C_h	=	hinge moment co-efficient
C_l	=	lift co-efficient of airfoil section
$C_{l\alpha}$	=	lift curve slope of airfoil
EA	=	axial stiffness
EI_{flap}	=	flap (transverse bending) stiffness
EI_{lag}	=	lag (in-plane bending) stiffness
GJ	=	torsion stiffness
I_{yy}, I_{zz}	=	principal mass moments of inertia of the blade cross-section
l	=	lift per unit span
r	=	radius of blade section
R	=	rotor radius
α_0	=	zero-lift angle of attack
δ	=	flap deflection angle
θ_0	=	collective pitch angle
ρ	=	density of air
λ	=	inflow ratio
Ω	=	rotational velocity

† School of Mechanical and Aerospace Engineering, Seoul National University, San 56-1, Sillim-Dong, Kwanak-Ku, Seoul 151-742, Republic of Korea
E-mail : anv.bala@gmail.com
Tel : 02-880-1901 , Fax : 02-887-2662

* School of Mechanical and Aerospace Engineering, Seoul National University

1. Introduction

Helicopters generally operate in a complex aerodynamic environment compared to a fixed wing aircraft. Due to the rotating blades, the flow speed will be different between the advancing and retreating sides of the rotor disk. Also, the wake vortices from the preceding blade impinge upon the following blade and this process is widely known as Blade Vortex Interaction (BVI). This unsteady aerodynamic environment induces significant vibratory loads at N times the rotor rotating frequency (N/rev) and aeroacoustic noise, where N is the total number of blades. Conventional rotor control system is incapable of handling such vibratory loads as the control is restricted to 1/rev. On the contrary, an active rotor varies the blade pitch with higher harmonic displacement using actuators based on conventional or advanced materials. Actuators based on piezoelectric materials are widely examined in recent years.

Active Trailing-edge Flap (ATF) has the advantage of low voltage input requirement and high control authority over other active control approaches. Active rotor blades developed using ATF are Smart Material Actuated Rotor Technology (SMART) active flap rotor[1, 2], the Active Blade Concept (ABC) rotor blade[3], and the Smart Hybrid Active Rotor Control System (SHARCS) rotor blade[4, 5, 6].

SNUF blade uses Amplified Piezoelectric Actuators (APA) for the flap actuation. APA is chosen considering its verified performance from earlier applications.

This paper presents the steps involved in the detailed design of SNUF blade viz., cross-section design, actuator and flap location selection, the load predictions carried out and stress-strain recovery analysis performed to verify the structural integrity.

2. Preliminary Design

2.1 Basic design requirements

SNUF blade design is derived from the existing NASA/ARMY/MIT Active Twist Rotor ATR[7] and SHARCS rotor blades. Basic properties of ATR and SHARCS rotor blades are summarized in Table 1.

Table 1 Properties of ATR and SHARCS blades

	ATR	SHARCS
Actuation method	Active twist	Hybrid
Rotor radius (cm)	139.7	109.6
Rotation speed (rpm)	687.5	1,555
Blade chord (mm)	108	80
Airfoil type	NACA 0012	NACA 0015
Tip Mach number	0.603	0.52
Lock number	4.55	5

Structural properties of the ATR blade are selected as target properties of SNUF blade. However, these properties need to be modified for the present testing condition. The differences in the testing conditions are explained in Section 3.1. Uniform cross-section and a linear built-in twist are chosen for simplicity. Flap deflection of ±4° is established as the criteria based on a previous ATF analysis[8]. The basic parameters of SNUF blade are summarized in Table 2.

Table 2 SNUF design configuration

Rotor type	Articulated
Rotor radius, R (cm)	128
Rotation speed (rpm)	1,528
Blade chord, c (cm)	10.24
Hinge offset (cm)	5.12
Root cutout (% span)	20
Airfoil type	NACA0012
Tip Mach number	0.60
Lock number	5.0
Mass per unit length (kg/m)	0.55
Pretwist (deg)	-10
Flap displacement	±4°

2.2 Cross-section design

For SNUF blade, a single spar configuration is chosen similar to that of ATR blade. Due to the non-availability of materials used in the ATR blade, the cross-section is designed with the available materials. The complicated front spar configuration of ATR blade is also replaced. The final design is shown in Figure 1. As compared in Table 3, the new design provides improved axial and flapwise bending stiffness. Apart from few discrepancies, considering the importance of axial, torsional stiffness and torsional response, it is decided to retain the current design. Ballast weights are added to maintain the center of gravity at 25% chord location.

Table 3 Cross-section properties

Property	Target Value	Design results
EA (N)	4.600×10^{6}	4.569×10^{6}
GJ (N-m^2)	6.800×10^{1}	6.810×10^{1}
EI_{flap} (N-m^2)	5.700×10^{1}	9.892×10^{1}
EI_{lag} (N-m^2)	1.900×10^{3}	2.237×10^{3}
Mass (kg/m)	5.500×10^{-1}	5.500×10^{-1}
I_{yy} (kg-m)	2.700×10^{-5}	6.252×10^{-6}
I_{zz} (kg-m)	2.250×10^{-4}	2.939×10^{-4}

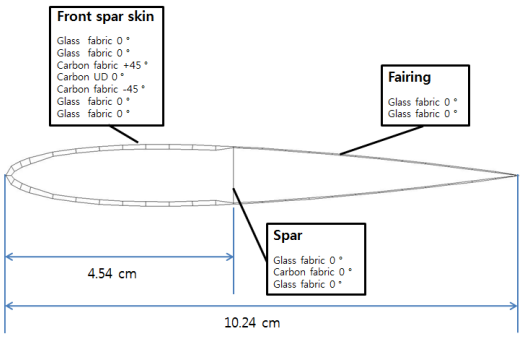

Figure 1 SNUF Cross-section Design

2.3 Built-in twist and flap location

A linear built-in twist distribution is chosen for the SNUF blade. The twist angle desired is -10°. But, due to the presence of flap axis, no twist is applied in the flap actuation region. The resulting built-in twist angle distribution is -8° as shown in Figure 2. Based on the

compromise between better aerodynamic control and low centrifugal force, the flap location is decided to be between 65%R to 85%R (Fig. 3).

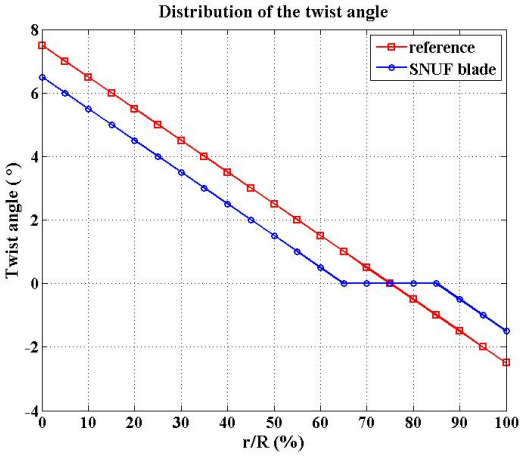

Figure 2 Built-in twist angle distribution

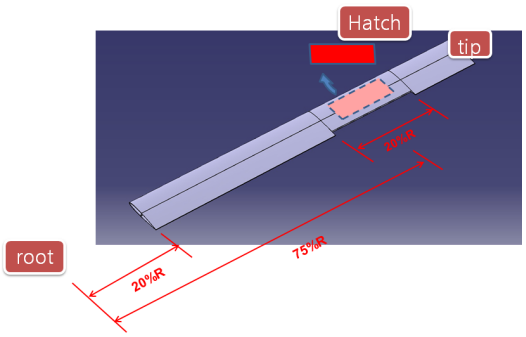

Figure 3 Spanwise design

2.3 Hinge moment

The flap hinge moment must be accurately predicted to determine the length of the required moment arm. Among the moments due to aerodynamic, inertial and centrifugal, it is important to estimate the trailing-edge flap hinge moment due to aerodynamic forces because of its larger magnitude[4]. A preliminary analytical calculation[9] is carried out for hover condition, by assuming uniform inflow and untwisted blades using blade element/momentum theory. The deflection of the trailing edge flap is considered through a change in the local effective angle of attack over the portion of the blade with flap. For a plain flap, the local lift for a blade with a deflected flap can be written as

$$l = \frac{1}{2}\rho(\Omega r)^2 c C_l \qquad (1)$$

where,

$$C_l = C_{l\alpha}\left(\theta_0 + \frac{\Delta\alpha_0}{\Delta\delta}\delta - \frac{\lambda\Omega R}{\lambda r}\right) \qquad (2)$$

The value of inflow ratio λ can be obtained by substituting the thrust co-efficient in terms of λ in the above equation and solving the quadratic equation. The hinge moment co-efficient and hinge moment per unit span can be determined using

$$C_h = \left(\frac{dC_h}{dC_l}\right)C_l + \left(\frac{dC_h}{d\delta}\right)\delta \qquad (3)$$

$$h = C_h \frac{1}{2}\rho(\Omega r)^2 c_f{}^2 \qquad (4)$$

Here, the value of $\frac{dC_h}{dC_l}, \frac{dC_h}{d\delta}$ and $\frac{\Delta\alpha_0}{\Delta\delta}$ can be found as functions of c_f / c. By substituting C_l in eqn. (3) from eqn. (2) and final C_h in eqn. (4) the hinge moment per unit span can be obtained. The final hinge moment can be obtained by integrating eqn. (4) over the flap span.

Hinge moment prediction is also carried out using a commercial CFD (Computational Fluid Dynamics) code for the forward flight condition. The 2-D blade model includes the flap and the parameters used for CFD analysis are tabulated in Table 4. The CFD results are corrected for compressibility based on Glauert factor. The magnitude of hinge moment based on analytical prediction for hover and CFD results for forward flight considering 4 degree flap deflection are tabulated in Table 5. However, for a more precise result unsteady aerodynamics has to be considered in the analytical prediction.

Table 4 Condition parameters used in the CFD calculation

Flap location	75%R
Flap length	20%R
Flap chord	15%c
Advance ratio (μ)	0.30
V (advancing side)	215 m/s
Mach number	0.63 (sea level)
Flap deflection (δ)	4 °
Fluid density (ρ)	1.225 kg/m^3 (sea level)
Temperature	300 °K
Flow condition	Incompressible, inviscid

Table 5 Hinge moment estimation ($\delta = 4^{o}$)

Flap Hinge Moment (N-m)			
Angle of Attack (°)	**CFD (Forward Flight)**	**Collective Pitch (°)**	**Analytical (Hover)**
0	0.0896	**0**	0.0538
5	0.1074	**5**	0.0652
10	0.1268	**10**	0.0843

2.4 Flap actuation region

The important factors considered in the selection of actuator are sufficient stroke, block force and most importantly smaller size. Based on these criteria, the APA 200M[10] is selected. The actual width of the actuator is decreased from 7 mm to 5 mm for SNUF blade. Further, a careful design of components for the flap actuation mechanism is necessary. Due to the rotating environment, it is better to use high specific strength materials to minimize and withstand the centrifugal load. Composites are considered initially, but ignored due to manufacturing complexities. Aluminium is used for the housing and fairing block (Fig 4). The push rod is made of steel to prevent buckling.

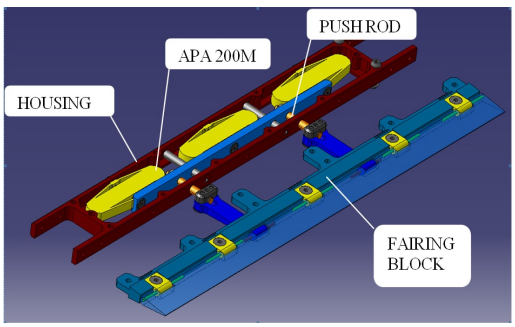

Figure 4 Flap actuation components

A schematic of the linkage mechanism is illustrated in Figure 5. To get the desired flap angle, an appropriate length of the moment arm (L2) is required. The block force of the APA 200M actuator is 73 while the free/maximum stroke of the actuator is 0.23 mm. The relation between L2 and the number of actuators is non-linear. The number of actuators is chosen after studying the relation between number of actuators, flap deflection angle and moment arm via a manual iterative process. According to Figure 6, the maximum flap deflection will be about ±3.4° and the optimum length of moment arm is 0.9 mm. Despite the insufficient flap deflection, considering the limitations in space and structural complexity, the three actuator configuration is finalized for examination.

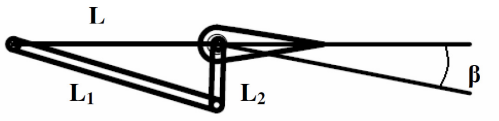

Figure 5 Linkage mechanism

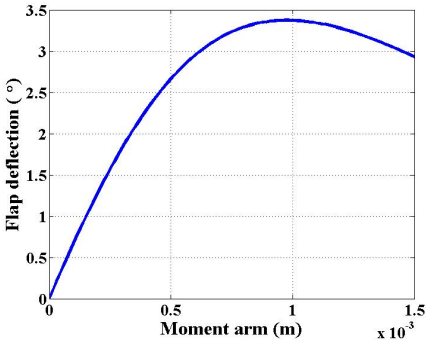

Figure 6 Flap deflection vs flap hinge moment arm length when three actuators are used

3. Detailed Design Analysis

3.1 Load predictions

The aerodynamic configuration of the SNUF blade is very similar to the ATR blade. However, the ATR blade is tested in a heavy gas environment, whereas, the SNUF blade will be tested in normal atmospheric condition. The normal rotation speed of ATR blade is 688 RPM. To match the tip Mach number value (0.6) of the ATR blade, the rotation speed of the SNUF blade is chosen as 1,528 RPM. Due to these differences, a precise prediction of loads for the SNUF blade is required again. A comprehensive rotorcraft analysis code, CAMRAD II[11], is used to predict the magnitude of the loads acting on the internal blade structure. The forward flight condition with the advance ratio of 0.3 is selected. The plots of the flap bending, lead-lag bending and torsion moments against the azimuth angle for the various radial locations are plotted in Figures 7(a), (b) and (c).

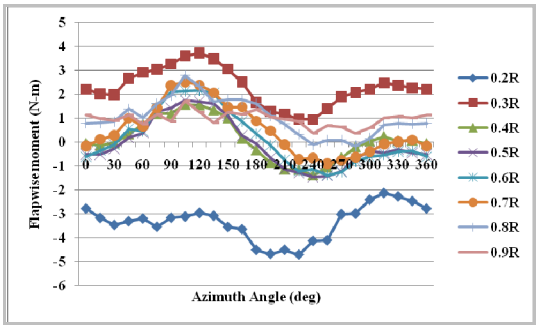

(a) Flapwise moment vs Azimuth angle

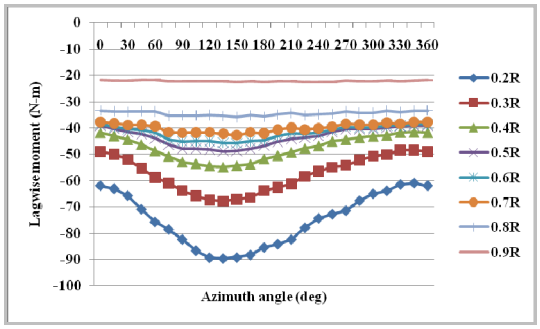

(b) Lagwise moment vs Azimuth angle

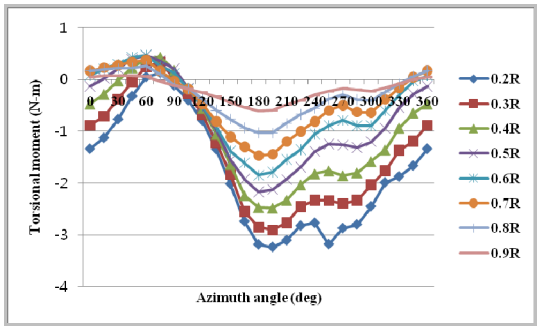

(c) Torsion moment vs Azimuth angle

Figures (a), (b) and (c) Aerodynamic moments vs azimuth angle at various radial locations

3.2 Stress/strain recovery analysis

SNUF blade rotates at relatively high speed i.e., 1,528 RPM. Also, there are relatively heavy components inside the blade. A careful stress/strain recovery analysis is required to evaluate the structural integrity of the blade. The centrifugal force is obtained by a one-dimensional geometrically exact beam analysis. A one-dimensional beam analysis can be conducted to estimate the loads existing on a reference line of the beam[12]. The largest magnitudes of the aerodynamic loads from CAMRAD II analysis as indicated in Figure 7 are extracted and combined with the centrifugal loads from 1-D beam analysis with a safety factor of 1.5.

The cross-section analysis results for the general section, which corresponds to the spanwise location without the flap and actuators, as obtained in Table 6, are used for the present stress/strain analysis. A stress/strain analysis is planned at 10 spanwise locations as indicated via a two-cell thin-walled analysis[13]. Details of the 10 spanwise locations considered are shown in Figure 8. However, as the root section is considered to be stiff enough and the stresses at tip are very small, the locations corresponding to 10% and 100% radii are neglected. The results of the present stress-strain recovery analysis are summarized in Table 7. Both the maximum stress and strain occur at the 30% radius location as illustrated in Figure 10. Numerical results indicate that the structure is unlikely to fail, as the maximum strain levels in all the plies are found to be lower than the allowable material strain levels. However, in order to make sure that the flap actuation region is also safe under the worst-case loading, a detailed three-dimensional finite element analysis will be carried out.

Table 6 Cross-section properties of the general section

Property	Design results
EA (N)	4.569×10^{6}
GJ (N-m^2)	6.810×10^{1}
EI_{flap} (N-m^2)	9.892×10^{1}
EI_{lag} (N-m^2)	2.237×10^{3}
Mass (kg/m)	5.644×10^{-1}
I_{yy} (kg-m)	16.769×10^{-6}
I_{zz} (kg-m)	5.434×10^{-4}

Table 7 Maximum strain results

Component	Max. strain (micro strain)	Existing/Allowable
longitudinal	11116.81	0.5387
transverse	3314.87	0.3994
shear	-2418.368	0.1812

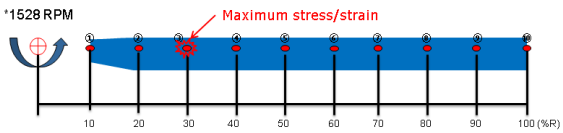

Figure 8 Spanwise location of the maximum strain

4. Conclusion

In this paper, the preliminary steps involved in designing an active trailing-edge flap blade intended to reduce vibration in helicopters are briefly explained. The cross-section is designed in such a way to ensure that the properties are close to target values from ATR rotor blades. The loads acting are predicting using comprehensive analysis program CAMRAD –II and a geometrically exact one-dimensional beam analysis. The stress-strain recovery analysis carried out using the predicted loads indicates that the structure is safe. Finally, the hinge moment is estimated using a basic analytical formulation. However, a three dimensional analysis and a more precise hinge moment prediction will be carried out for better understanding of the structural behavior and to ensure the desired flap actuation respectively.

References

(1) Straub, F. K., Kennedy, D. K., Domzalski, D. B., Hassan, A. A., Ngo, H., Anand, V., and Birchette, T., 2004,Smart Material Actuated Rotor Technology - SMART, Journal of Intelligent Material Systems and Structures, Vol. 15, pp. 249~260.

(2) Straub, F. K., Kennedy, D. K., Stemple, A. D., Anand, V. R. and Birchette, T. S., 2004, Development and whirl tower test of the SMART active flap rotor, SPIE's Intl. Symposium on Smart Structures and Materials, San Diego, CA.

(3) Mainz, H., van der Wall, B. G., Leconte, P., Ternoy, F. and des Rochettes, H. M., 2005, ABC Rotor Blades: Design, Manufacturing and Testing, 31st European Rotorcraft Forum, Florence, Italy.

(4) Nitzsche, F., Feszty, D., Waechter, D., Bianchi, E., Voutsinas, S., Gennaretti, M., Coppotelli, G. and Ghiringhelli, G.L., 2005, The SHARCS project: Smart Hybrid Active Rotor Control System for Noise and Vibration Attenuation of Helicopter Rotor Blades, 31st European Rotorcraft Forum, pp. 52-1-52-15.

(5) Feszty, D., Nitzsche, F., Khomutov, K., and Lynch, B, K., "Design and Instrumentation of the SHARCS Scaled Rotor with Three Independent Control Systems," American Helicopter Society 64th Annual Forum, Montreal, Canada, 2008.

(6) Feszty, D., Nitzsche, F., Cha, M., Khomutov, K., Lynch, B., Mander, A., Oxley, G., Poirier, P., and Ulker, F. D.,2007, SHARCS: Smart Hybrid Active Rotor Control System Design Report, SHARCS Report No. 004.

(7) Shin S. J., 2001, Integral Twist Actuation of Helicopter Rotor Blades for Vibration Reduction, PhD Thesis, Aeronautics and Astronautics Dept., Massachusetts Institute of Technology, Cambridge, MA, USA.

(8) Park, J. S., Kim, T. S., and Shin, S. J., 2007, Design and Aeroelastic Analysis of Advanced Active flap Blades Utilizing Single Crystal Piezoelectric Actuators, International Forum on Rotorcraft Multidisciplinary Technology, Seoul, Korea.

(9) Lee T., 1999, High Displacement Piezoelectric Trailing-Edge Flap Mechanism for Helicopter Rotors, PhD Thesis, Dept. of Aerospace Eng., University of Maryland, College Park, USA.

(10) Cedrat Ltd., http://www.cedrat.com/ [cited 9/2009]

(11) Johnson, W., 1998, Rotorcraft Dynamic Models for a Comprehensive Analysis, American Helicopter Society International 54th Annual Forum Proceedings, Washington, DC, May 20-22, pp. 452-471.

(12) Shang, X., and Hodges, D. H., 1995, Aeroelastic Stability of Composite Rotor Blades in Hover, Proceedings of the 36th Structures, Structural Dynamics and Materials Conference, New Orleans, Louisiana.

(13) Shin, S. -J., 1999, Design, Manufacturing and Testing of an Active Twist Rotor, Master's Thesis, Massachusetts Institute of Technology.